Environmental Science & Technology

pubs.acs.org/est

Article

Preventing Aerosol Emissions in a CO_2 Capture System: Combining Aerosol Formation Inhibition and Wet Electrostatic Precipitation

Lingyu Shao, Chang Liu, Yifan Wang, Zhengda Yang, Zhicheng Wu, Feng Xu, You Zhang, Yu Ni, Chenghang Zheng,* and Xiang Gao

Cite This: *Environ. Sci. Technol.* 2022, 56, 16167−16177

Read Online

ACCESS | Metrics & More | Article Recommendations

ABSTRACT: Aerosol emission from the CO_2 capture system has raised great concern for causing solvent loss and serious environmental issues. Here, we propose a comprehensive method for reducing aerosol emissions in a CO_2 capture system under the synergy of aerosol formation inhibition and wet electrostatic precipitation. The gas−solvent temperature difference plays a vital role in aerosol formation, with aerosol emissions of 740.80 mg/m^3 at 50 K and 119.36 mg/m^3 at 0 K. Different effects of SO_2 and SO_3 on aerosol formation are also found in this research; the aerosol mass concentration could reach 2341.25 mg/m^3 at 20 ppm SO_3 and 681.01 mg/m^3 at 50 ppm SO_2 with different aerosol size distributions. After the CO_2 capture process, an aerosol removal efficiency of 98% can be realized by electrostatic precipitation under different CO_2 concentrations. Due to the high concentration of aerosols and aerosol space charge generated by SO_2 and SO_3, the removal performance of the wet electrostatic precipitator decreases, resulting in a high aerosol emission concentration (up to 130.26 mg/m^3). Thus, a heat exchanger is installed before the electrostatic precipitation section to enhance aerosol growth and increase aerosol removal efficiency. Under the synergy of aerosol formation inhibition and electrostatic precipitation, an aerosol removal efficiency of 99% and emission concentrations lower than 5 mg/m^3 are achieved, contributing to global warming mitigation and environmental protection.

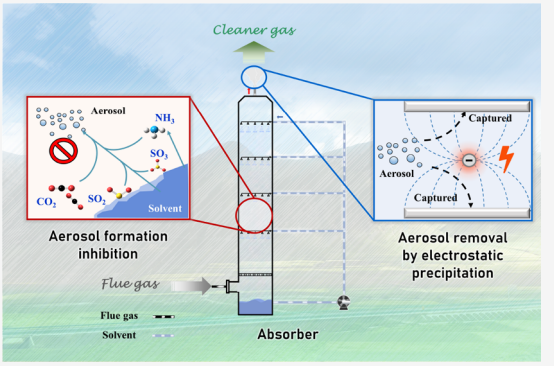

KEYWORDS: *environmental pollution, CO_2 capture, aerosol, solvent, electrostatic precipitation*

INTRODUCTION

Global warming and climate change are global concerns of the current era and are mainly caused by increasing greenhouse gas (GHG) emissions.[1] Carbon dioxide, as the major anthropogenic GHG, accounted for 72% of the total emissions in 2019.[2] Carbon capture, utilization, and storage has been considered a promising and necessary technology for reducing CO_2 emissions and contributing to achieving carbon neutrality.[3,4] Recently, amine scrubbing has become a promising large-scale CO_2 capture technology due to its high capture efficiency, mature process, and good compatibility.[5,6] However, some solvents and their degradation products are discharged with the flue gas while the CO_2 capture system operates.[7] These emissions lead to solvent loss and a series of environmental problems.[8]

During the typical amine scrubbing process, mainly for a monoethanolamine (MEA) solution, the solvent will be carried by flue gas due to its inherent volatility and gas−liquid temperature difference, resulting in solvent loss at approximately 0.21−3.65 kg/t CO_2.[9] In addition to solvent emissions, many kinds of organic pollutants produced by oxidative degradation and thermal degradation, such as ammonia, aldehydes, and ketones,[10] will also be discharged into the atmosphere along with the flue gas. The increased cost of decarbonization and unexpected environmental pollution will be caused by the abovementioned phenomena. Generally, the pollutant emissions after an absorber can be divided into vapor-type and aerosol-type emissions.[11] Aerosol emissions are usually generated by heterogeneous and homogeneous vapor condensation and have been reported from both pilot plants and bench experiments, which were found to be important emission sources and have drawn increasing concerns.[12−14] In addition, it is worth mentioning that mist formation depends to a high extent on the presence of condensation nuclei, such as particulate matter, soot, SO_2, NO_x, and H_2SO_4.[15] These fine particles contribute to heterogeneous nucleation, which is a dominant mechanism of aerosol formation in most industrial gas cleaning processes. Significant amine emissions can occur from

Received: June 10, 2022
Revised: October 5, 2022
Accepted: October 5, 2022
Published: October 17, 2022

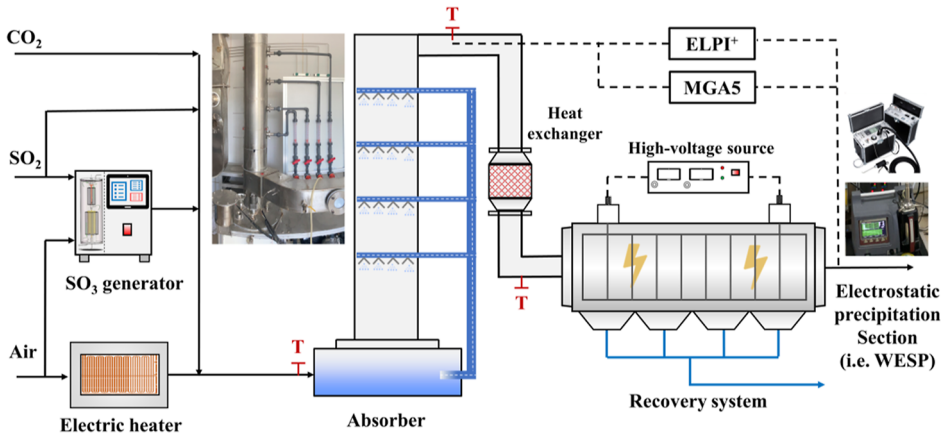

Figure 1. Schematic diagram of the experimental system.

aerosols under certain conditions. Kamijo et al. found that the addition of 0−3 ppm SO_3 corresponds to 0.8−67.5 ppm MEA emissions in a 1 t/day CO_2 capture system.[16] Khakharia's work shows that the total emissions of MEA reach 1200−1900 mg/m^3 with an aerosol concentration of 1.4−1.7 × 10^8 1/cm^3.[17] Moreover, the combined capture of SO_2 and CO_2[18,19] from flue gas has already received attention from numerous commercial and research organizations and carried out commercial-scale projects (e.g., the CASPER process developed by the Netherlands Organization for Applied Scientific Research),[20] where the impact of high concentrations of sulfur oxides on aerosol formation cannot be ignored. Thus, inhibiting the formation of aerosols during the absorption process has been considered a method to reduce aerosol emissions.

Recently, to reduce the emission of amines and volatile degradation products, washing systems such as water washing sections,[16] acid washing,[21] and demisters[22] have been applied. The water wash column and mist eliminator are common decarbonized flue gas treatment equipment in the CO_2 capture system. Mitsubishi Heavy Industries proposed a multistage water wash system for amine emission, which realized a 25% reduction in solvent consumption and lower amine emission.[23] An acid wash was also designed by Aker Clean Carbon, achieving ammonia emission falling from 4 to 1 ppm and decreasing the emission of degradation products such as dimethylamine and methylamine.[21] Moreover, Moser et al. developed a novel control technology called a "dry bed" with lower water consumption, which could reduce pollutant emissions by one magnitude.[24] However, there are still problems with the current technology that limit promotion. For example, the cost of the acid wash is still high, and the removal efficiency of water wash and mist eliminator on aerosol is limited due to its inherently small particle size (d_p < 10 μm).[25,26] Therefore, a high-efficiency aerosol emission control method should be taken into account, which is crucial to less solvent loss and pollution in the CO_2 capture process.

Aerosol removal by electrostatic precipitation, which shows excellent fine particle removal performance in flue gas, is considered the most effective method for aerosol collection.[27,28] This method has been successfully applied in various flue gas treatment devices, such as a wet electrostatic precipitator (WESP), which is utilized to reduce SO_3/sulfuric acid aerosol concentrations in ultralow emission systems. In our previous study,[29] aerosol removal was intensively studied, achieving an outlet concentration below 1 mg/m^3. However, the particle-capturing mechanism of electrostatic precipitation is inefficient for particles in the size range of 0.1−1 μm because of the inherent low electrical mobility.[30] Research has indicated that cooling-enhanced vapor condensation can be a feasible means of improving the removal of fine particles.[31−34] In addition, in the CO_2 capture system, some researchers applied WESP before the absorber to remove the condensation nuclei with 99% removal efficiency.[35] However, the existence of SO_2 would generate sulfuric acid aerosol under the effect of corona discharge,[36] which would increase the aerosol emission of the absorber. Reviewing previous studies, a full process aerosol emission control method by combining aerosol formation inhibition and aerosol removal after CO_2 absorption can be possible and has not been further investigated.

In this study, a comprehensive aerosol emission control method was proposed by combining aerosol formation inhibition and electrostatic precipitation. Additionally, we investigated aerosol formation under the effect of operation parameters and sulfuric oxides, as well as aerosol removal efficiencies. This research is essential for the development of the CO_2 capture system and pollutant control technologies.

MATERIALS AND METHODS

Experimental System. The laboratory-scale system simulated a complete CO_2 capture and exhaust gas purification process, as illustrated in Figure 1. The diagram mainly consists of four main sections: (1) simulated gas generation, (2) absorber, (3) electrostatic precipitator section, and (4) aerosol measurement. The main stream of the simulated flue gas was produced by an induced fan, and the gas temperature was raised to approximately 333−363 K by an electric heater with a gas flow rate of 40 m^3/h. A generator was installed to produce SO_3 by SO_2 catalytic oxidation.[37,38] The generator was maintained at approximately 683 K to promote SO_3 conversion efficiency. Afterward, the gas entered the absorber with CO_2/SO_2/SO_3 mixed.

The absorber was designed with a four-stage spray and was equipped with a perforated sieve plate. The liquid−gas ratio of the absorber was kept at 20 L/m^3, and the lean solvent was newly configured before every experiment. The temperature of the lean solvent was controlled at 313−333 K by the electric heater at the bottom of the absorber, while it was 313 K unless otherwise specified.

In the electrostatic precipitation section, a 10-wire discharge electrode was applied for simultaneous aerosol charging and

https://doi.org/10.1021/acs.est.2c04181
Environ. Sci. Technol. 2022, 56, 16167−16177

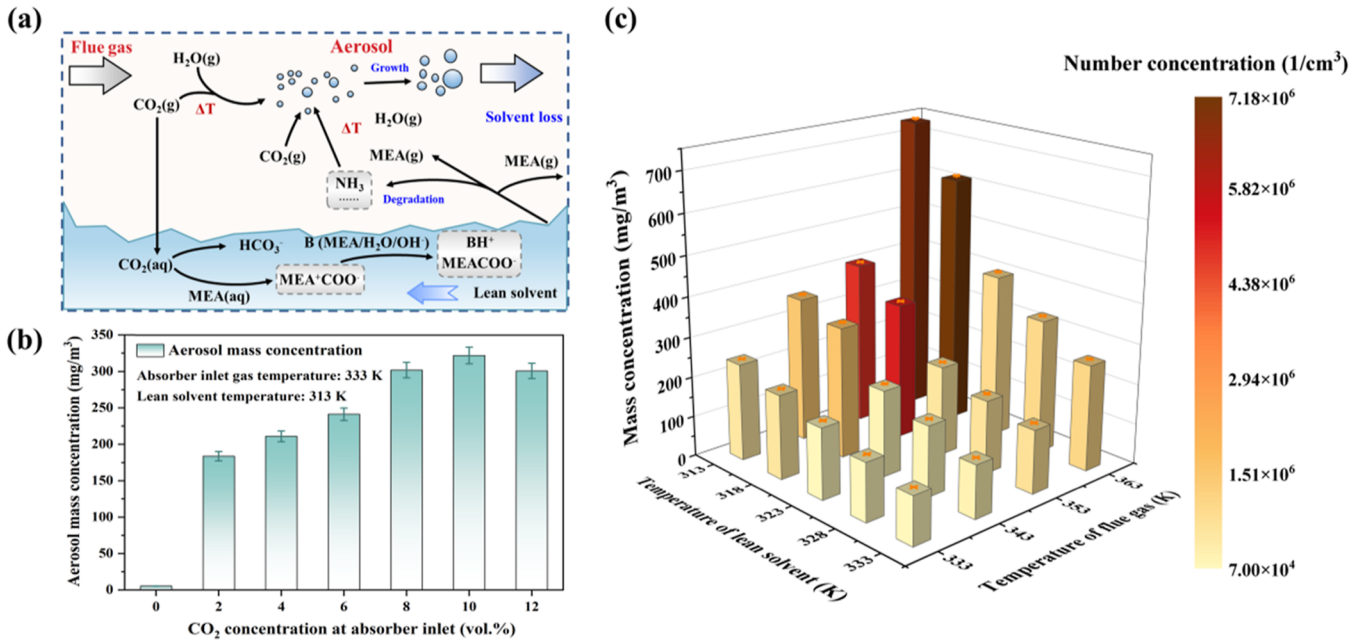

Figure 2. (a) Schematic of aerosol formation in the absorber, (b) change in aerosol mass concentration under the effect of CO_2 concentrations, and (c) change in aerosol formation under the effect of gas and lean solvent temperature (with 10 vol % CO_2).

collection. The wire interval was 100 mm, and the distance between the wire and the collection plate was 60 mm. Rod discharge electrodes with a 2 mm diameter and a high-frequency power source (40 kV, 20 kHz, and negative DC) were used for the corona discharge. The discharge electrode was inserted into two Teflon insulators for position fixing and electrical insulation. The insulator surface was heated to eliminate the potential of vapor condensation. The collection plates were made of stainless steel 1200 mm in length and 300 mm in height. After the process of aerosol charging, the charged aerosol was captured on the surface of the collection plates and cleaned by a water film. In addition, the water would carry the fugitive solvent after the spraying process, providing the potential for solvent loss reduction.

Experimental and Analytical Methods. *Chemicals and Materials.* All chemicals were commercially available and directly used without further purification. MEA (>99%, Macklin Biochemical Co., Ltd., China) was used to prepare an aqueous solution of 4 mol/L MEA with deionized water. CO_2 (>99%, Linan Gas Co., Ltd., China) and SO_2 (>99%, Linan Gas Co., Ltd., China) were supplied to the experimental system.

Aerosol Measurement. Due to the submicron or nanoscale size of the aerosol generated from the absorber,[7,39] the electrical low-pressure impactor (ELPI$^+$, Dekati Ltd., Finland) was chosen to measure the concentration and size distribution of the aerosol, which has been proven to be reliable for aerosol (e.g., sulfuric acid aerosol, sulfate aerosol, etc.) measurements by many researchers worldwide.[40−42] The impactor provided real-time (10 Hz) data on aerosol number and mass concentration with 14 size fractions. The sampling system temperature was kept constant with the flue gas temperature to ensure accuracy of aerosol measurements. Besides, a single-stage diluter (Diluter DI-1000, Dekati Ltd., Finland) was utilized to dilute the flue gas at a dilution ratio of 1:8. Prior to normal investigation, the accuracy of the measurement was evaluated. Five repeated measurements were taken under the same conditions, with a sampling time of 60 s for each measurement.

In this research, the aerosol size distribution is expressed as dp − dn/dlogd_p, which can be represented by the following equation

$$\mathrm{d}n/\mathrm{dlog}d_p = \frac{\Delta n}{\log d_{i,up} - \log d_{i,low}} \quad (1)$$

where n is the number concentration (cm^{-3}) of the aerosol, d_p is the diameter (μm) of the aerosol, and $d_{i,up}$ and $d_{i,low}$ represent the upper and lower diameters (μm) for a certain size range, respectively.

In addition, the median size was calculated from aerosol number concentration and the growth of aerosols was represented, to some extent, with the relative median size ($\overline{d}_{outlet}/\overline{d}_{inlet}$). The mean diameter was calculated by the arithmetic mean of the number distribution as follows

$$\overline{d} = \frac{\sum n_i d_i}{n} \quad (2)$$

The aerosol removal efficiency was calculated with the aerosol mass concentration as follows

$$\eta = 1 - \frac{m_{outlet}}{m_{inlet}} \quad (3)$$

$$m(d_i) = n(d_i)\frac{\pi\rho_p}{6}d_i^3 \quad (4)$$

$$m = \sum m(d_i) \quad (5)$$

where m_{outlet} and m_{inlet} represent the aerosol mass concentrations (mg/m^3) of the outlet and inlet measured by ELPI$^+$, respectively, and ρ_p is the assumed spherical aerosol density.

Gas Analysis. For the measurement of CO_2 and SO_2, a nondispersive infrared multigas analyzer (MGA 5, MRU, Germany) was used to measure the CO_2/SO_2 concentration at the absorber outlet. To avoid the condensation of water vapor in the measurement system, the probe was heated to 423 K with

https://doi.org/10.1021/acs.est.2c04181
Environ. Sci. Technol. 2022, 56, 16167−16177

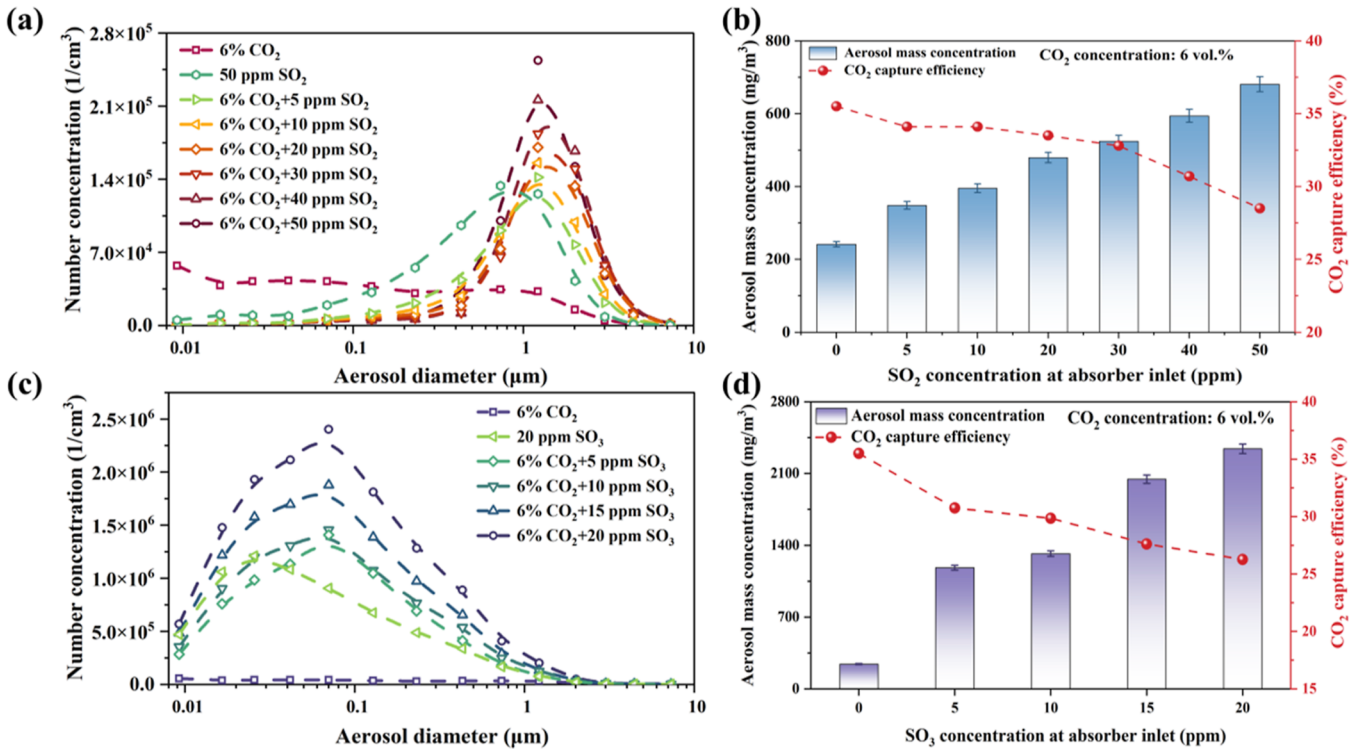

Figure 3. (a) Aerosol size distribution under the effect of SO_2 at the absorber outlet, (b) change in the aerosol mass concentration and CO_2 capture efficiency under the effect of SO_2, (c) aerosol size distribution under the effect of SO_3 at the absorber outlet, and (d) change in the aerosol mass concentration and CO_2 capture efficiency under the effect of SO_3.

the sampling line heated to 393 K. The concentration of SO_3 was converted based on the concentration of SO_2 at the inlet of the generator, with the conversion efficiency from SO_2 to SO_3 supposed to be nearly 100% since no residual SO_2 could be detected at the exit of the generator.[29,37,38]

RESULTS AND DISCUSSION

Aerosol Formation Inhibition. Inhibiting the formation of aerosols in the absorber is the most direct way to reduce solvent loss. Aerosol formation involves homogeneous and heterogeneous condensation, as well as mass transfer and chemical reactions between the aerosol−gas phase.[26] In this process, supersaturation of the gas phase, which is affected by temperature and partial pressures of condensable components, is an important factor in the formation of an aerosol and its growth. Thus, the effect of both flue gas temperature and solvent temperature and gas composition on aerosol formation should be studied for aerosol formation inhibition.

Adjusting Operation Parameters. During the process of CO_2 absorption, a high supersaturation is realized due to the spray and gas temperature drop, resulting in water−vapor condensation in the absorber. CO_2, amine vapor formed by volatilization, and degradation products (e.g., NH_3) would transfer into the aerosol faster due to the higher specific surface area of aerosol than solvent. Khakharia et al. proposed that the amine in the aerosol would react with CO_2 rapidly and form a nonvolatile carbamate or bicarbonate, which reduced the amine volatility in the aerosols.[17] Therefore, gaseous amines would condense continuously on the aerosol. The hygroscopicity of aerosols was enhanced due to the accumulation of amines and CO_2 in the aerosols, leading to aerosol growth. Figure 2a shows the aerosol formation process during CO_2 absorption. Based on the abovementioned analysis, inhibition of condensation and gas-aerosol mass transformation could be a potential method.

The chemical reaction in the absorber can significantly promote heterogeneous condensation and accelerate the mass transfer of solvent to aerosol. Figure 2b indicates the change in aerosol mass concentration under different CO_2 concentrations. The results showed that the aerosol mass concentration at the absorber outlet increased with the CO_2 concentration. The aerosol mass concentration reached 322.17 mg/m^3. Aerosol emissions were almost undetectable when the CO_2 concentration was 0 vol %. However, when the CO_2 concentration reached 12 vol %, the mass concentration (300.95 mg/m^3) decreased compared to that at 10 vol %, which was similar to the trend obtained by Khakharia et al.[17] This phenomenon can be attributed to the fact that there were two competing effects with increasing CO_2 concentration. On the one hand, when the CO_2 concentration increased, the amount of CO_2 captured by the liquid also increased, leading to lower activity and thus lower volatility of the solvent. On the other hand, a more violent chemical reaction released more heat, resulting in a temperature increase in the absorber and thus the volatility of solvent enhancement. Both these effects lead to a change in the supersaturation profile in the absorber and thereby a change in aerosol emission.

Generally, the process of aerosol formation involves homogeneous and heterogeneous condensation, which could be driven by supersaturation. The temperature of flue gas and solvent are the key factors that affect supersaturation.[43] A higher gas−liquid temperature difference would increase the temperature gradient along with the absorber, and then the supersaturation of the gas phase increased, causing more vapor to condense on aerosols. Moreover, at higher solvent temperatures, the equilibrium partial pressure of the volatile components

https://doi.org/10.1021/acs.est.2c04181
Environ. Sci. Technol. 2022, 56, 16167−16177

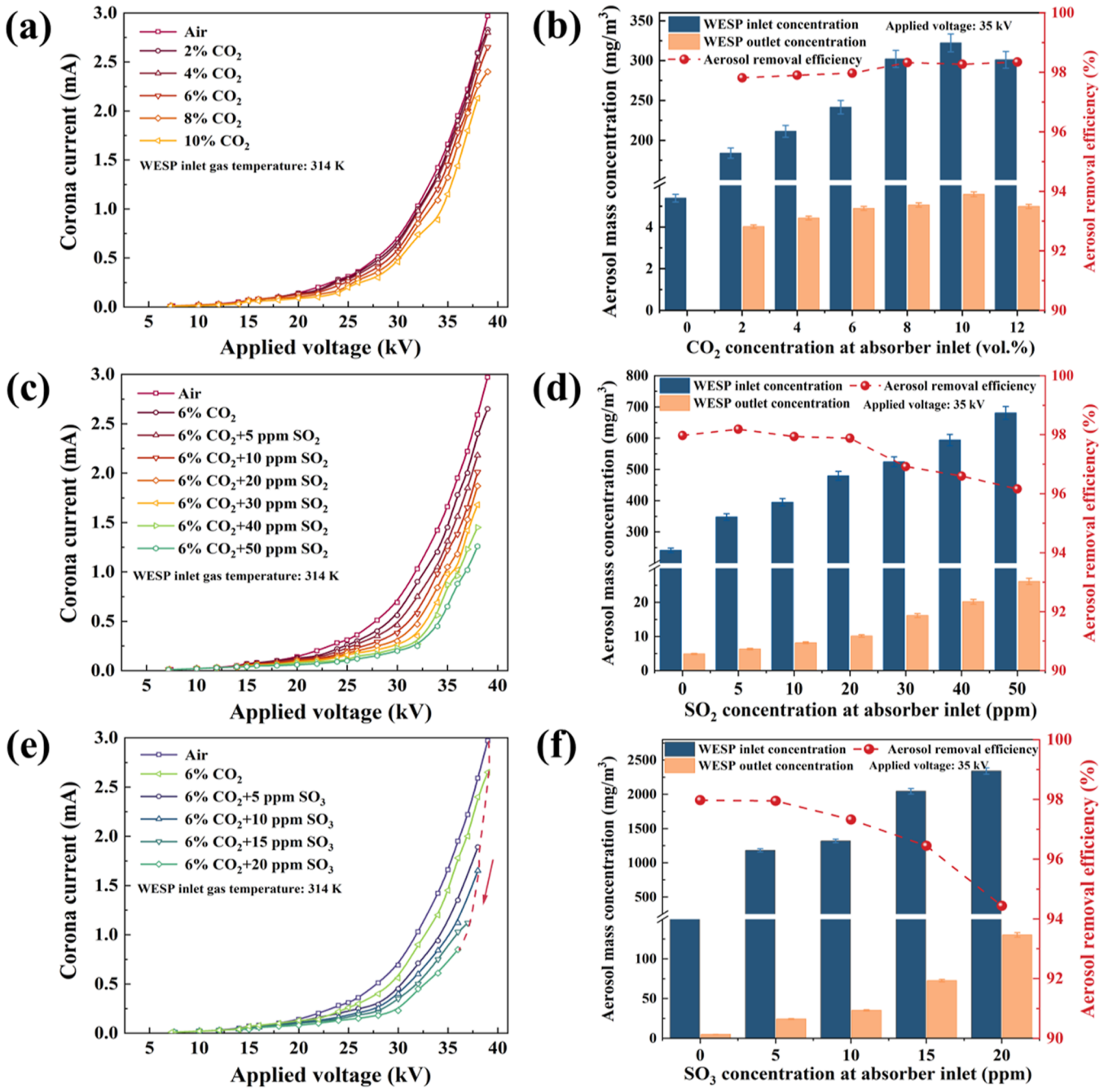

Figure 4. (a) Corona discharge characteristics under different CO_2 concentrations, (b) aerosol removal performance under different CO_2 concentrations, (c) corona discharge characteristics under different SO_2 concentrations, (d) aerosol removal performance under different SO_2 concentrations, (e) corona discharge characteristics under different SO_3 concentrations, and (f) aerosol removal performance under different SO_3 concentrations.

increased, leading to a decrease in the supersaturation of the gas phase and an inhibition in aerosol growth by condensation. As shown in Figure 2c, the aerosol emission increased with the gas−liquid temperature difference. When the temperature difference reached 50 K, the aerosol mass concentration reached 740.80 mg/m^3 with a number concentration of 7.16×10^6 $1/cm^3$, which was 6.21 times that of no temperature difference (119.36 mg/m^3). The flue gas would be cooled in the absorber. At the same solvent temperature, the higher flue gas temperature leads to a larger temperature gradient in the absorber, which would enhance the condensation of the condensable components, thus increasing the aerosol emission. In addition, prior studies have shown that aerosol emissions decrease as lean solvent temperatures rise, whereas vapor emissions increase, as increased solvent temperature results in more volatile solvents transferring to the gas phase.[13,17,44]

Effect of SO_2 and SO_3. Compared with CO_2, sulfur oxides are more likely to react with the solvent and thus promote the mass transfer of the amine vapor to the aerosol phase. Figure 3 displays the effects of SO_2 (0−50 ppm) and SO_3 (0−20 ppm) on aerosol formation and CO_2 capture efficiency.

As shown in Figure 3a, the presence of SO_2 would significantly increase the aerosol number concentration. Considering the flue gas desulfurization in power plants and the combined capture of

https://doi.org/10.1021/acs.est.2c04181
Environ. Sci. Technol. 2022, 56, 16167−16177

SO_2 and CO_2, the SO_2 concentration was set to range from 0 to 50 ppm in this experiment. When 50 ppm SO_2 was added to flue gas mixed with 6 vol % CO_2, the total number concentration reached 6.13×10^5 1/cm^3, which was an increase of 48.43% compared with 6 vol % CO_2 only. Interestingly, after the addition of SO_2, more aerosols focalized in size approximately 1 μm, indicating that amounts of aerosols were obviously coagulated. This phenomenon can be ascribed to the fact that amine oxidative degradation could be enhanced by the addition of SO_2,[26,45] leading to the formation of more degradation products in aerosols and the transfer of more amines to aerosols. The mechanism of aerosol formation under the effect of SO_2 will be further investigated in our future research. Moreover, the aerosol mass concentration at the absorber outlet increased with the SO_2 concentration. The aerosol mass concentration was 681.01 mg/m^3 with 50 ppm SO_2 and 6 vol % CO_2, which was 2.82 times that of 6 vol % CO_2 only (as shown in Figure 3b). In addition, SO_2 is considered an impurity to impede the performance and chemical stability of CO_2 absorbents, which will lead to a decrease in CO_2 capture efficiency.[46,47] As shown in Figure 3b, the CO_2 capture efficiency was reduced to 28.5% with the increase in SO_2 concentration.

A prior study showed that SO_3 could cause higher levels of amine emissions in CO_2 capture systems. SO_3 is transformed into sulfuric acid aerosol in high-humidity gas by homogeneous condensation during the spray process.[26,48] Owing to the temperature cooling down at the absorber column, the MEA present in the gas phase condenses on the sulfuric acid aerosol nuclei rather than in the bulk liquid phase, which causes high amine emissions. In this study, the aerosol size distribution under the effect of SO_3 was investigated (as shown in Figure 3c). Noticeably, the total number concentration of aerosols after SO_3 addition (1.31×10^7 1/cm^3) was nearly two orders of magnitude higher than that of only 6 vol % CO_2. Comparing the aerosol size distribution with the condition of 20 ppm SO_3 only, the results showed that the formation of aerosol in this part was closely related to the sulfuric acid aerosol. More obvious aerosol growth occurred under the synergistic effect of SO_3 and CO_2. More aerosols formed with increasing SO_3 concentration and focalized in size by approximately 0.07 μm. For the mass concentration (as shown in Figure 3d), after adding SO_3, the aerosol emission reached more than 1000 mg/m^3, and an aerosol emission of 2341.25 mg/m^3 was found at a SO_3 concentration of 20 ppm (with 6 vol % CO_2). Besides, a decrease in CO_2 capture efficiency was found with the increase of SO_3 concentration. Similar to the effects of SO_2, the SO_3 with more acidic limited the reaction between CO_2 and the absorbent. Moreover, more solvent loss made less absorbent to be used for CO_2 capture, leading to a decrease in CO_2 capture efficiency.[16]

Consequently, in view of the obvious promotion of aerosol formation by SO_2 and SO_3, pre-scrubbing and other pretreatment technologies for sulfur oxide reduction before the gas enters the absorber should be considered to inhibit aerosol formation. According to the abovementioned study, aerosol formation inhibition by regulating operating parameters such as flue gas temperature, solvent temperature, and pretreatment of flue gas components that can potentially promote aerosol formation could be considered.

Aerosol Removal by Electrostatic Precipitation. Previous studies have illustrated that WESP demonstrated good performance in the removal of sulfuric acid aerosols. Thus, in this section, a heat exchanger and an electrostatic precipitation section were applied for aerosol removal after the absorber under different conditions.

Prior to the investigation of the co-benefits of combining the heat exchanger and electrostatic precipitation, the aerosol removal performance of only electrostatic precipitation was explored (as shown in Figure 4). CO_2, as a part of the inert atmosphere, would affect the corona discharge characteristic of the device. As shown in Figure 4a, the corona current decreased slightly with an increase in CO_2 concentration under the same applied voltage, and the spark-over voltage decreased from 39 to 38.3 kV with a CO_2 concentration of 10 vol %. Furthermore, the aerosol removal performance is illustrated in Figure 4b. To obtain a good and comparable removal performance, the applied voltage was selected as 35 kV. The results indicated that the aerosol removal efficiency was maintained at approximately 98% with an outlet concentration lower than 5 mg/m^3. Noticeably, the change in CO_2 concentration did not significantly affect the removal efficiency.

Under the condition of flue gas with SO_2, the corona current decreased (from 2.59 to 1.26 mA, at 38 kV) with an increase in SO_2 concentration under the same applied voltage (shown in Figure 4c). The reduction of the corona current can be attributed to the decreasing ionization rate between electrons and gas molecules because of the increased electronegativity of the SO_2 molecule. Part of the SO_2 was converted to SO_3 under corona discharge, which could also suppress corona discharge. Therefore, the aerosol removal efficiency decreased with increasing SO_2 concentration (from 97.97 to 96.15%, as shown in Figure 4d). The aerosol mass concentration at the electrostatic precipitation section outlet was kept at 26.15 mg/m^3 with 50 ppm SO_2 and 6.31 mg/m^3 with 5 ppm SO_2.

The electric field and ion density were seriously affected by the space charge of sulfuric acid aerosol transformed by SO_3. Some application results indicated that corona discharge would be inhibited in the presence of high-concentration sulfuric acid aerosol. What is more, ion-induced nucleation under the effect of electrostatic field and SO_2/SO_3[49,50] leads to an increase in aerosol number concentration and inhibition of corona discharge, further contributing to the lower removal efficiency. Figure 4e displays the corona discharge characteristics under the effect of SO_3. The results showed that SO_3 had negative effects on corona discharge. The maximum corona current decreased from 2.97 to 0.65 mA when the SO_3 concentration increased from 0 to 20 ppm. The spark-over voltage decreased from 39 to 36 kV due to the increasing SO_3 concentration. Consequently, the aerosol removal efficiency decrease occurred under the effect of SO_3 (from 97.97 to 94.43%, as shown in Figure 4f).

Considering the decrease in removal efficiency caused by high aerosol concentrations, methods need to be proposed to neutralize the reduction in electrostatic precipitation efficiency. First, efficient removal of sulfur oxides is necessary before CO_2 capture, for example, more efficient desulphurization and prewashing with alkaline solutions before absorber. Then, some means of reducing aerosol concentration at the inlet of wet electrostatic precipitation devices (such as water washing, mesh-type demister, etc.) should also be taken into account. What is more, the main reason for the reduction of aerosol removal efficiency is the insufficient charge of aerosol caused by the decrease of corona current. Therefore, the use of spike-type electrodes and a combined pre-charger can effectively improve the removal efficiency of high-concentration aerosol.[51]

Aerosol Removal Enhancement by Temperature Management. Numerous studies have shown that the removal of

https://doi.org/10.1021/acs.est.2c04181
Environ. Sci. Technol. 2022, 56, 16167−16177

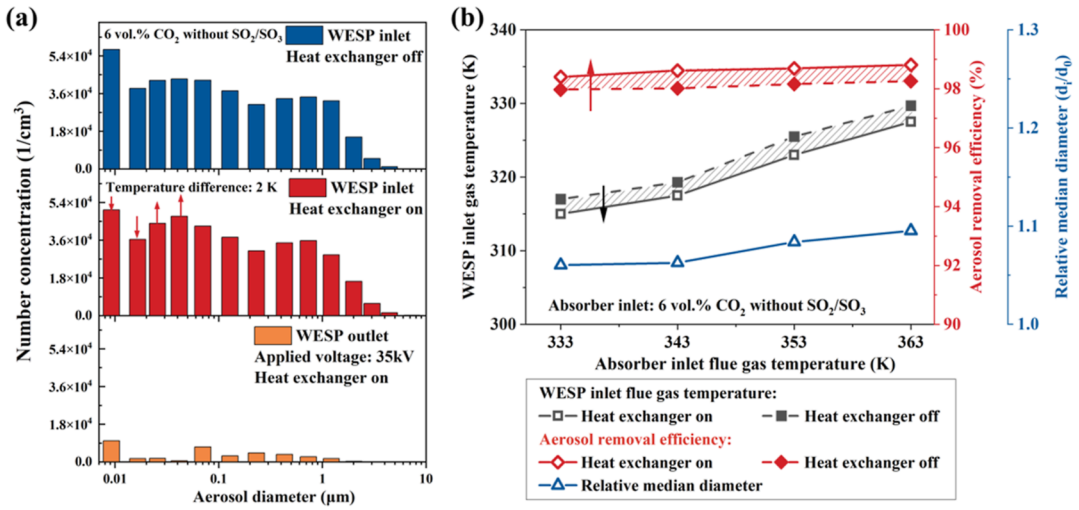

Figure 5. (a) Aerosol growth by temperature management and (b) aerosol removal enhancement by combining temperature management and electrostatic precipitation.

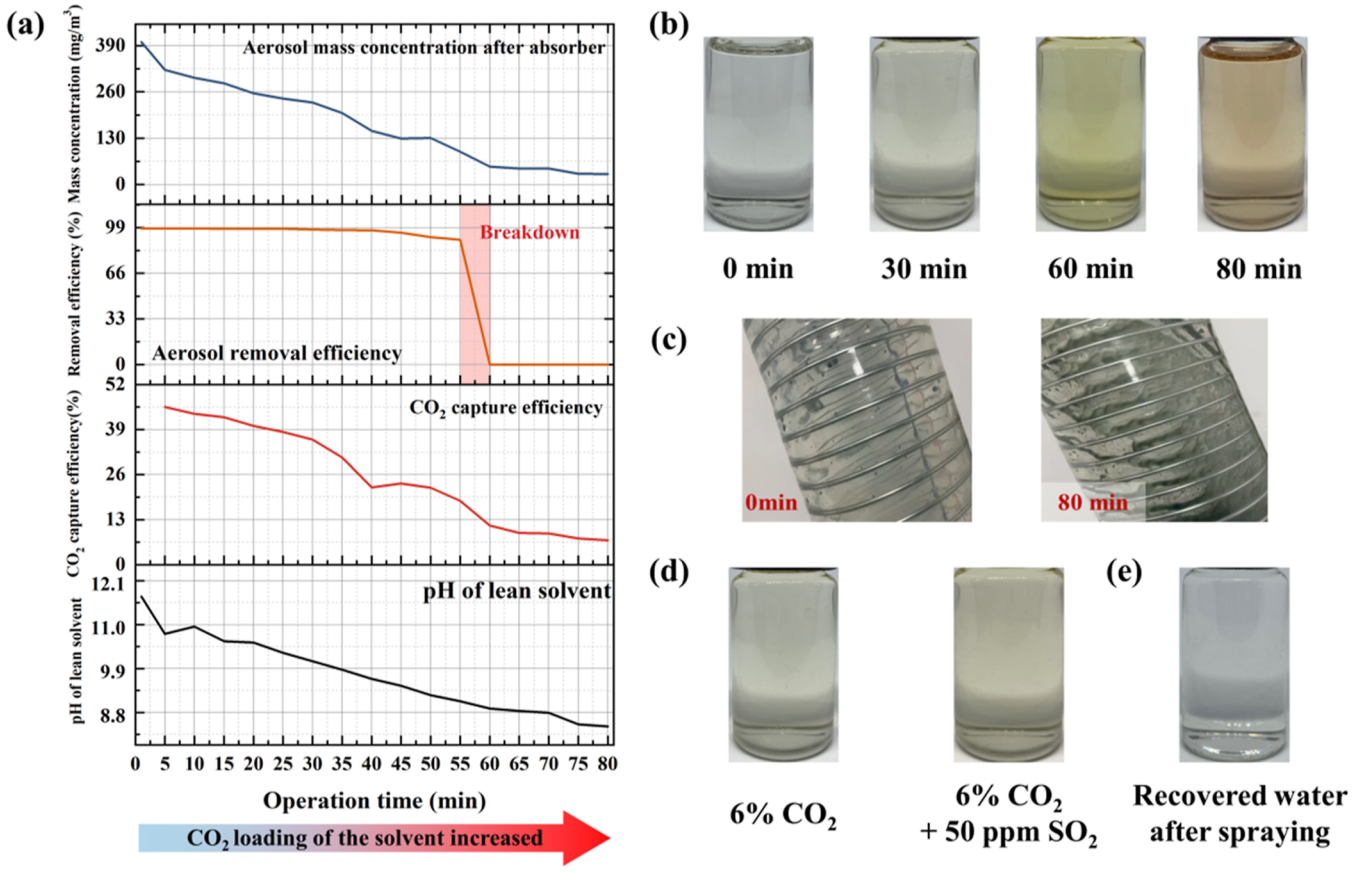

Figure 6. (a) Change in parameters under long-term operation without desorption, (b) appearance of solvent deterioration during operation, (c) attachment of droplets in the experimental system, (d) solvent deterioration caused by other pollutants, and (e) appearance of the electrostatic precipitation section cleaning water.

aerosols is significantly affected by aerosol size.[52] Based on the mechanism of aerosol growth, the change in flue gas temperature would substantially affect the condensation process of water vapor, thereby affecting the growth of aerosols and removal efficiency. Thus, a heat exchanger with water cooling was installed before the electrostatic precipitation section to further improve the removal efficiency of aerosols. Apparently, after temperature management, the number of aerosols in the 0.009−0.017 μm range decreased, while the number of aerosols in the 0.026−0.042 μm range increased (shown in Figure 5a), indicating aerosol growth after heat exchange. In addition, aerosols larger than 1 μm were almost all removed, whereas aerosols of 0.1−1 μm remained in the electrostatic precipitation section outlet. Figure 5b shows the aerosol removal enhancement by temperature management under different flue gas temperatures. Due to the effect of gas cooling, the flue gas

https://doi.org/10.1021/acs.est.2c04181
Environ. Sci. Technol. 2022, 56, 16167−16177

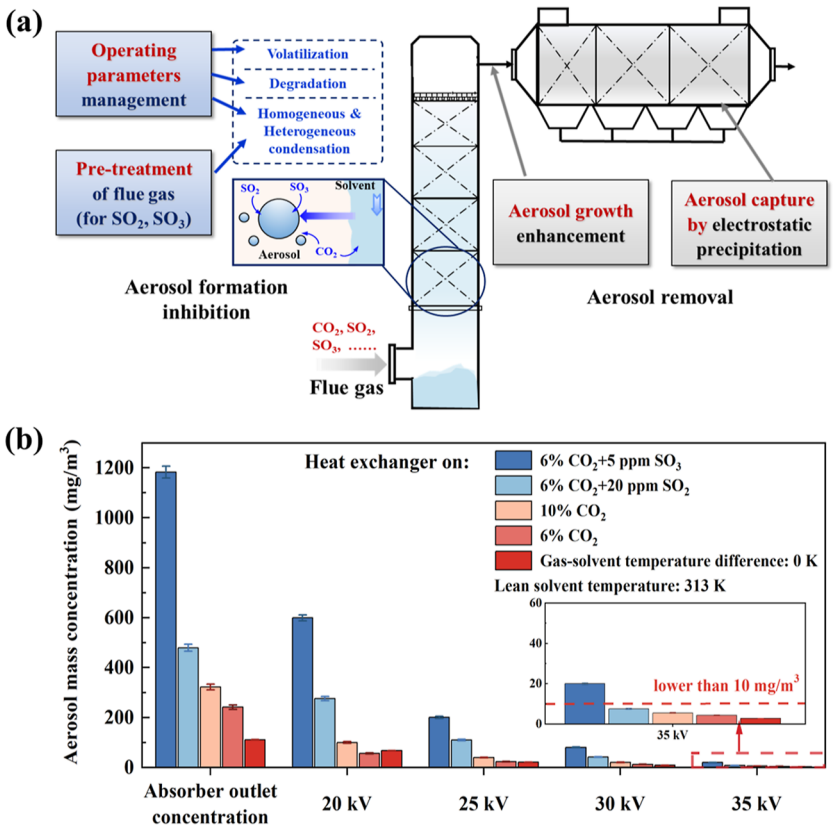

Figure 7. (a) Schematic of the comprehensive aerosol emission control method and (b) aerosol removal performance after combining aerosol formation inhibition and wet electrostatic precipitation.

temperature decreased by approximately 2 K, and the aerosol size increased by 6−8%, achieving an aerosol removal efficiency of 98.40−98.81%.

Challenges and Suggestions for the Treatment Method. In practice, the CO_2 loading of the solvent would increase with cycling before desorption, which was also found to have an impact on aerosol emissions in the study by Yi et al.[7] Additionally, the accumulation of aerosols in the electrostatic precipitation section as the operating time increases can have an impact on the operation of the aerosol removal device. Thus, this section explores the changes in absorber aerosol emissions with increasing CO_2 loading conditions and the changes in the electrostatic precipitation section over long-term operation.

A solvent with high CO_2 loading usually has lower amine volatility and reactivity, which slows amine transfer and the heat release of the reaction. As indicated in Figure 6a, as the solvent circulated within the absorber, the CO_2 loading of the solvent increased and solvent loss (involving volatilization and degradation) occurred, leading to a noticeable drop in the pH of the solvent, which in turn resulted in a reduction in CO_2 capture efficiency and aerosol emission. Thus, desorption is necessary after a period of operation. In addition, properly increasing the lean solvent CO_2 loading might be a viable and effective method of controlling amine emissions. However, the CO_2 capture rate also decreases due to the decrease in the absorbing ability of the solvent. This method needs to be used in combination with other absorption enhancement methods, such as increasing the liquid−gas ratio. Moreover, with the accumulation of aerosol on the electrodes and collection plates due to its inherent high viscosity (Figure 6c), the stability of device operation also needs attention in future research, such as developing suitable cleaning methods or choosing a higher electrode temperature.

The degradation of the solvent also occurred and could be inferred from the color of the solvent (Figure 6b), which was based on catalysis by metal ions dissolved from the absorber, organic compounds, and a combination of both. In addition, the presence of acidic gases cannot be ignored, as they have a tendency to catalyze the oxidation of amines, as SO_2 seemed to increase the rate of oxidation of MEA with an increase in its concentration (Figure 6d). Thus, solvent management technologies, reclaiming by ion exchange, and pretreatment of other acidic gases should be considered for further application. Furthermore, the solvent recovery from electrostatic precipitation cleaning water could be taken into account for reducing solvent loss in the future (Figure 6e).

In addition, the desorption process can lead to more significant solvent volatilization and thermal degradation due to its higher temperatures, resulting in solvent losses and the formation of large amounts of aerosols as a result of gas cooling after stripping, which will also need to be investigated in depth in the future.

In general, different from the removal of dust in flue gas, the removal of aerosols from the CO_2 capture process by electrostatic precipitation requires more consideration. Here are some suggestions:

i Considering the decreased removal efficiency due to high aerosol concentrations found in the experiments, applying the spike electrode and reducing the wire-plate distance appropriately can be taken into account to enhance aerosol charging and migration.

https://doi.org/10.1021/acs.est.2c04181
Environ. Sci. Technol. 2022, 56, 16167−16177

ii Considering that the interaction of amine with metals leads to solvent degradation and equipment corrosion, corrosion-resistant materials can be applied for the electrodes and collection plates.

iii Considering the absorber size and space-saving requirement, the vertical electrostatic precipitation device can be applied. Combining it with the water washing tower can be a better choice for enhancing pollutant removal and reducing spray-water consumption.

Aerosol Emission Control by Combining Aerosol Formation Inhibition and Wet Electrostatic Precipitation. According to the results in Figure 4, in some cases, especially for flue gas with SO_2 or SO_3, there were still limits in controlling the emission of aerosols only by electrostatic precipitation. Thus, it is necessary to inhibit the formation of aerosols in the absorber by adjusting the operating parameters or pretreating the sulfur oxides before the absorber and then remove the discharged aerosols by combining the heat exchanger and wet electrostatic precipitation to realize effective aerosol emission control in the CO_2 capture system (shown in Figure 7a). The aerosol removal performance after combining the aerosol formation inhibition and electrostatic precipitation is indicated in Figure 7b, achieving aerosol emissions below 10 mg/m^3 in most cases. In particular, an aerosol mass concentration lower than 5 mg/m^3 was realized by decreasing the gas-solvent temperature difference. However, further treatment technology was needed due to the impact of SO_3 (electrostatic precipitator outlet concentration: 19.93 mg/m^3).

Overall, aerosol emissions in the CO_2 capture system play a vital role in solvent loss and lead to serious environmental impacts; thus, how to control aerosol emissions during CO_2 capture should be specifically considered in the future-oriented design of the CO_2 capture system to realize lower carbon emission without any environmental pollution. In this study, aerosol emissions under the influence of flue gas/solvent temperature, CO_2 concentration, and SO_2/SO_3 concentration were tested and the highest emission could reach 2341.25 mg/m^3. Thus, this research proposed a comprehensive aerosol emission control method by combining aerosol formation inhibition and wet electrostatic precipitation, which could realize an aerosol removal efficiency of over 99% and emission concentrations lower than 5 mg/m^3.

This study provides possible recommendations for reducing solvent loss and pollutant emission from the CO_2 capture system. In future studies, the formation mechanism of aerosols in complex flue gas composition (CO_2, SO_2, SO_3, etc.) during CO_2 capture or combined capture of SO_2 and CO_2 process will be focused on. Aerosol emissions under different absorbents will also be studied in the future. Besides, novel devices based on electrostatic precipitation for removing high-viscosity and high-concentration aerosols (e.g., a vertical WESP in combination with the water washing tower) could be considered to cope with the complex operating conditions in the future.

AUTHOR INFORMATION

Corresponding Author

Chenghang Zheng − *State Key Lab of Clean Energy Utilization, State Environmental Protection Engineering Center for Coal-Fired Air Pollution Control, Zhejiang University, Hangzhou 310027, P. R. China; Jiaxing Research Institute, Zhejiang University, Jiaxing 314000, P. R. China;* Email: zhengch2003@zju.edu.cn

Authors

Lingyu Shao − *State Key Lab of Clean Energy Utilization, State Environmental Protection Engineering Center for Coal-Fired Air Pollution Control, Zhejiang University, Hangzhou 310027, P. R. China*

Chang Liu − *State Key Lab of Clean Energy Utilization, State Environmental Protection Engineering Center for Coal-Fired Air Pollution Control, Zhejiang University, Hangzhou 310027, P. R. China*

Yifan Wang − *State Key Lab of Clean Energy Utilization, State Environmental Protection Engineering Center for Coal-Fired Air Pollution Control, Zhejiang University, Hangzhou 310027, P. R. China*

Zhengda Yang − *College New Energy, China University of Petroleum East China, Qingdao 266580, P. R. China*

Zhicheng Wu − *State Key Lab of Clean Energy Utilization, State Environmental Protection Engineering Center for Coal-Fired Air Pollution Control, Zhejiang University, Hangzhou 310027, P. R. China*

Feng Xu − *State Key Lab of Clean Energy Utilization, State Environmental Protection Engineering Center for Coal-Fired Air Pollution Control, Zhejiang University, Hangzhou 310027, P. R. China*

You Zhang − *State Key Lab of Clean Energy Utilization, State Environmental Protection Engineering Center for Coal-Fired Air Pollution Control, Zhejiang University, Hangzhou 310027, P. R. China*

Yu Ni − *China Power Engineering Consulting Group Co., Ltd., Beijing 100120, P. R. China*

Xiang Gao − *State Key Lab of Clean Energy Utilization, State Environmental Protection Engineering Center for Coal-Fired Air Pollution Control, Zhejiang University, Hangzhou 310027, P. R. China;* orcid.org/0000-0002-1732-2132

Complete contact information is available at: https://pubs.acs.org/10.1021/acs.est.2c04181

Notes

The authors declare no competing financial interest.

ACKNOWLEDGMENTS

This work was supported by the National Natural Science Foundation of China (no. 52076191 and no. 51906258) and Key Research & Development Plan of Shandong Province (no. 2020CXGC011401).

REFERENCES

(1) Yoro, K. O.; Daramola, M. O.CO_2 emission sources, greenhouse gases, and the global warming effect. In *Advances in Carbon Capture*; Rahimpour, M. R., Farsi, M., Makarem, M. A., Eds.; Woodhead Publishing, 2020; Chapter 1, pp 3−28.

(2) Olivier, J. G. J.*Trends in Global CO_2 and Total Greenhouse Gas Emissions*; PBL Netherlands Environmental Assessment Agency: Netherlands, 2017.

(3) Lv, B.; Guo, B.; Zhou, Z.; Jing, G. Mechanisms of CO_2 Capture into Monoethanolamine Solution with Different CO_2 Loading during the Absorption/Desorption Processes. *Environ. Sci. Technol.* **2015**, *49*, 10728−10735.

(4) Tang, H.; Zhang, S.; Chen, W. Assessing Representative CCUS Layouts for China's Power Sector toward Carbon Neutrality. *Environ. Sci. Technol.* **2021**, *55*, 11225−11235.

(5) Rochelle, T. Amine Scrubbing for CO_2 Capture. *Science* **2009**, *325*, 1652−1654.

(6) Orlov, A. A.; Demenko, D. Y.; Bignaud, C.; Valtz, A.; Marcou, G.; Horvath, D.; Coquelet, C.; Varnek, A.; de Meyer, F. Chemoinformatics-

Driven Design of New Physical Solvents for Selective CO_2 Absorption. *Environ. Sci. Technol.* **2021**, *55*, 15542−15553.
(7) Yi, N.; Fang, M.; Di, W.; Xia, Z.; Wang, T.; Wang, Q. Aerosol Emissions of Amine-Based CO_2 Absorption System: Effects of Condensation Nuclei and Operating Conditions. *Environ. Sci. Technol.* **2021**, *55*, 5152−5160.
(8) Nielsen, C.; D'Anna, B.; Karl, M.; Aursnes, M.; Boreave, A.; Bossi, R.; Bunkan, A.; Glasius, M.; Hallquist, M.; Hansen, A.-M.; Kristensen, K.; Mikoviny, T.; Maguta, M. M.; Müller, M.; Nguyen, Q.; Westerlund, J.; Salo, K.; Skov, H.; Stenstrøm, Y.; Wisthaler, A.Atmospheric Degradation of Amines (ADA). *Summary Report: Photo-Oxidation of Methylamine, Dimethylamine and Trimethylamine*. CLIMIT project no. 201604, 2011.
(9) Moser, P.; Wiechers, G.; Schmidt, S.; Garcia Moretz-Sohn Monteiro, J.; Charalambous, C.; Garcia, S.; Sanchez Fernandez, E. Results of the 18-month test with MEA at the post-combustion capture pilot plant at Niederaussem − new impetus to solvent management, emissions and dynamic behaviour. *Int. J. Greenh. Gas Control* **2020**, *95*, 102945.
(10) Vega, F.; Sanna, A.; Navarrete, B.; Maroto-Valer, M. M.; Cortés, V. J. Degradation of amine-based solvents in CO_2 capture process by chemical absorption. *Greenhouse Gases: Sci. Technol.* **2014**, *4*, 707−733.
(11) Wei, C.-C.; Puxty, G.; Feron, P. Amino acid salts for CO_2 capture at flue gas temperatures. *Chem. Eng. Sci.* **2014**, *107*, 218−226.
(12) Maree, Y.; Nepstad, S.; de Koeijer, G. Establishment of Knowledge base for Emission Regulation for the CO_2 Technology Centre Mongstad. *Energy Proc.* **2013**, *37*, 6265−6272.
(13) Khakharia, P.; Brachert, L.; Mertens, J.; Huizinga, A.; Schallert, B.; Schaber, K.; Vlugt, T. J. H.; Goetheer, E. Investigation of aerosol based emission of MEA due to sulphuric acid aerosol and soot in a Post Combustion CO_2 Capture process. *Int. J. Greenh. Gas Control* **2013**, *19*, 138−144.
(14) Fujita, K.; Muraoka, D.; Ogawa, T.; Kitamura, H.; Suzuki, K.; Saito, S. Evaluation of amine emissions from the post-combustion CO_2 capture pilot plant. *Energy Proc.* **2013**, *37*, 727−734.
(15) Spietz, T.; Chwoła, T.; Krótki, A.; Tatarczuk, A.; Więcław-Solny, L.; Wilk, A. Ammonia emission from CO_2 capture pilot plant using aminoethylethanolamine. *Int. J. Environ. Sci. Technol.* **2018**, *15*, 1085−1092.
(16) Kamijo, T.; Kajiya, Y.; Endo, T.; Nagayasu, H.; Tanaka, H.; Hirata, T.; Yonekawa, T.; Tsujiuchi, T. SO_3 Impact on Amine Emission and Emission Reduction Technology. *Energy Proc.* **2013**, *37*, 1793−1796.
(17) Khakharia, P.; Brachert, L.; Mertens, J.; Anderlohr, C.; Huizinga, A.; Fernandez, E. S.; Schallert, B.; Schaber, K.; Vlugt, T. J. H.; Goetheer, E. Understanding aerosol based emissions in a Post Combustion CO_2 Capture process: Parameter testing and mechanisms. *Int. J. Greenh. Gas Control* **2015**, *34*, 63−74.
(18) Qi, G.; Wang, S.; Xu, Z.; Zhao, B.; Chen, C. Mass transfer and kinetics study on combined CO_2 and SO_2 absorption using aqueous ammonia. *Int. J. Greenh. Gas Control* **2015**, *41*, 60−67.
(19) Yang, J.; Yu, X.; An, L.; Tu, S.-T.; Yan, J. CO_2 capture with the absorbent of a mixed ionic liquid and amine solution considering the effects of SO_2 and O_2. *Appl. Energy* **2017**, *194*, 9−18.
(20) Misiak, K.; Sanchez, C. S.; van Os, P.; Goetheer, E. Next Generation Post- combustion Capture: Combined CO_2 and SO_2 Removal. *Energy Proc.* **2013**, *37*, 1150−1159.
(21) Knudsen, J. N.; Bade, O. M.; Anheden, M.; Bjorklund, R.; Gorset, O.; Woodhouse, S. Novel Concept for Emission Control in Post Combustion Capture. *Energy Proc.* **2013**, *37*, 1804−1813.
(22) Khakharia, P.; Kvamsdal, H. M.; da Silva, E. F.; Vlugt, T. J. H.; Goetheer, E. Field study of a Brownian Demister Unit to reduce aerosol based emission from a Post Combustion CO_2 Capture plant. *Int. J. Greenh. Gas Control* **2014**, *28*, 57−64.
(23) Hirata, T.; Nagayasu, H.; Yonekawa, T.; Inui, M.; Kamijo, T.; Kubota, Y.; Tsujiuchi, T.; Shimada, D.; Wall, T.; Thomas, J. Current Status of MHI CO_2 Capture Plant technology, 500 TPD CCS Demonstration of Test Results and Reliable Technologies Applied to Coal Fired Flue Gas. *Energy Proc.* **2014**, *63*, 6120−6128.
(24) Moser, P.; Schmidt, S.; Stahl, K.; Vorberg, G.; Lozano, G. A.; Stoffregen, T.; Rösler, F. Demonstrating Emission Reduction − Results from the Post-combustion Capture Pilot Plant at Niederaussem. *Energy Proc.* **2014**, *63*, 902−910.
(25) de Cazenove, T.; Bouma, R. H. B.; Goetheer, E. L. V.; van Os, P. J.; Hamborg, E. S. Aerosol Measurement Technique: Demonstration at CO_2 Technology Centre Mongstad. *Energy Proc.* **2016**, *86*, 160−170.
(26) Majeed, H.; Svendsen, H. F. Effect of water wash on mist and aerosol formation in absorption column. *Chem. Eng. J.* **2018**, *333*, 636−648.
(27) Xu, Y. S.; Liu, X. W.; Cui, J.; Chen, D.; Xu, M. H.; Pan, S. W.; Zhang, K.; Gao, X. P. Field Measurements on the Emission and Removal of $PM_{2.5}$ from Coal-Fired Power Stations: 4. PM Removal Performance of Wet Electrostatic Precipitators. *Energy Fuels* **2016**, *30*, 7465−7473.
(28) Anderlohr, C.; Brachert, L.; Mertens, J.; Schaber, K. Collection and Generation of Sulfuric Acid Aerosols in a Wet Electrostatic Precipitator. *Aerosol Sci. Technol.* **2015**, *49*, 144−151.
(29) Yang, Z. D.; Zheng, C. H.; Zhang, X. F.; Chang, Q. Y.; Weng, W. G.; Wang, Y.; Gao, X. Highly efficient removal of sulfuric acid aerosol by a combined wet electrostatic precipitator. *RSC Adv.* **2018**, *8*, 59−66.
(30) Wang, Y.; Gao, W.; Zhang, H.; Shao, L.; Wu, Z.; Li, L.; Sun, D.; Zheng, C.; Gao, X. Enhanced particle precipitation from flue gas containing ultrafine particles through precharging. *Process Saf. Environ. Prot.* **2020**, *144*, 111−122.
(31) Yin, J.; Zhang, J.; Lv, L.; Zhong, H. Heterogeneous condensation for high concentration of insoluble submicron particles under magnetic field. *Powder Technol.* **2022**, *398*, 117145.
(32) Zheng, C.; Shao, L.; Wang, Y.; Zheng, H.; Gao, W.; Zhang, H.; Wu, Z.; Shen, J.; Gao, X. Investigation of the growth and removal of particles in coal-fired flue gas by temperature management. *Fuel* **2021**, *302*, 121220.
(33) Shao, L.; Wang, Y.; Zhou, C.; Yang, Z.; Gao, W.; Wu, Z.; Li, L.; Yang, Y.; Yang, Y.; Zheng, C.; Gao, X. Co-Benefits of Pollutant Removal, Water, and Heat Recovery from Flue Gas through Phase Transition Enhanced by Corona Discharge. *Environ. Sci. Technol.* **2022**, *56*, 8844−8853.
(34) Wu, H.; Pan, D.; Jiang, Y.; Huang, R.; Hong, G.; Yang, B.; Peng, Z.; Yang, L. Improving the removal of fine particles from desulfurized flue gas by adding humid air. *Fuel* **2016**, *184*, 153−161.
(35) Mertens, J.; Anderlohr, C.; Rogiers, P.; Brachert, L.; Khakharia, P.; Goetheer, E.; Schaber, K. A wet electrostatic precipitator (WESP) as countermeasure to mist formation in amine based carbon capture. *Int. J. Greenh. Gas Control* **2014**, *31*, 175−181.
(36) Yang, Z. D.; Zheng, C. H.; Zhang, X. F.; Li, C. J.; Wang, Y.; Weng, W. G.; Gao, X. Sulfuric Acid Aerosol Formation and Collection by Corona Discharge in a Wet Electrostatic Precipitator. *Energy Fuels* **2017**, *31*, 8400−8406.
(37) Zheng, C.; Zheng, H.; Shen, J.; Gao, W.; Yang, Z.; Zhao, Z.; Wang, Y.; Zhang, H.; Gao, X. Evolution of Condensable Fine Particle Size Distribution in Simulated Flue Gas by External Regulation for Growth Enhancement. *Environ. Sci. Technol.* **2020**, *54*, 3840−3848.
(38) Yang, Z.; Zheng, C.; Li, Q.; Zheng, H.; Zhao, H.; Gao, X. Fast Evolution of Sulfuric Acid Aerosol Activated by External Fields for Enhanced Emission Control. *Environ. Sci. Technol.* **2020**, *54*, 3022−3031.
(39) Gupta, V.; Mobley, P.; Tanthana, J.; Cody, L.; Barbee, D.; Lee, J.; Pope, R.; Chartier, R.; Thornburg, J.; Lail, M. Aerosol emissions from water-lean solvents for post-combustion CO_2 capture. *Int. J. Greenh. Gas Control* **2021**, *106*, 103284.
(40) Mertens, J.; Brachert, L.; Desagher, D.; Thielens, M. L.; Khakharia, P.; Goetheer, E.; Schaber, K. ELPI+ measurements of aerosol growth in an amine absorption column. *Int. J. Greenh. Gas Control* **2014**, *23*, 44−50.
(41) Ngohang, F.-E.; Fontaine, G.; Gay, L.; Bourbigot, S. Smoke composition using MLC/FTIR/ELPI: Application to flame retarded ethylene vinyl acetate. *Polym. Degrad. Stab.* **2015**, *115*, 89−109.

https://doi.org/10.1021/acs.est.2c04181
Environ. Sci. Technol. 2022, 56, 16167−16177

(42) Fdez-Arroyabe, P.; Salcines, C.; Kassomenos, P.; Santurtún, A.; Petäjä, T. Electric charge of atmospheric nanoparticles and its potential implications with human health. *Sci. Total Environ.* **2022**, *808*, 152106.
(43) Schaber, K.; Körber, J.; Ofenloch, O.; Ehrig, R.; Deuflhard, P. Aerosol formation in gas−liquid contact devices—nucleation, growth and particle dynamics. *Chem. Eng. Sci.* **2002**, *57*, 4345−4356.
(44) Nguyen, T.; Hilliard, M.; Rochelle, G. T. Amine volatility in CO_2 capture. *Int. J. Greenh. Gas Control* **2010**, *4*, 707−715.
(45) Uyanga, I. J.; Idem, R. O. Studies of SO_2- and O_2-Induced Degradation of Aqueous MEA during CO2 Capture from Power Plant Flue Gas Streams. *Ind. Eng. Chem. Res.* **2007**, *46*, 2558−2566.
(46) Gao, J.; Wang, S.; Zhao, B.; Qi, G.; Chen, C. Pilot-Scale Experimental Study on the CO_2 Capture Process with Existing of SO_2: Degradation, Reaction Rate, and Mass Transfer. *Energy Fuels* **2011**, *25*, 5802−5809.
(47) Liu, C.; Zhao, Z.; Shao, L.; Zhu, L.; Xu, F.; Jiang, X.; Zheng, C.; Gao, X. Experimental study and modified modeling on effect of SO_2 on CO_2 absorption using amine solution. *Chem. Eng. J.* **2022**, *448*, 137751.
(48) Zheng, C.; Wang, Y.; Liu, Y.; Yang, Z.; Qu, R.; Ye, D.; Liang, C.; Liu, S.; Gao, X. Formation, transformation, measurement, and control of SO_3 in coal-fired power plants. *Fuel* **2019**, *241*, 327−346.
(49) Sorokin, A.; Arnold, F.; Wiedner, D. Formation and growth of sulfuric acid−water cluster ions: Experiments, modelling, and implications for ion-induced aerosol formation. *Atmos. Environ.* **2006**, *40*, 2030−2045.
(50) Borra, J. P. Charging of aerosol and nucleation in atmospheric pressure electrical discharges. *Plasma Phys. Controlled Fusion* **2008**, *50*, 124036.
(51) Yang, Z.; Zheng, C.; Liu, S.; Guo, Y.; Liang, C.; Wang, Y.; Hu, D.; Gao, X. A combined wet electrostatic precipitator for efficiently eliminating fine particle penetration. *Fuel Process. Technol.* **2018**, *180*, 122−129.
(52) Wu, H.; Pan, D.; Bao, J.; Jiang, Y.; Hong, G.; Yang, B.; Yang, L. Improving the removal efficiency of sulfuric acid droplets from flue gas using heterogeneous vapor condensation in a limestone-gypsum desulfurization process. *J. Chem. Technol. Biotechnol.* **2017**, *92*, 230−237.

https://doi.org/10.1021/acs.est.2c04181
Environ. Sci. Technol. 2022, 56, 16167−16177